

INTERACTIONS BETWEEN ENDOTHELIA OF THE TRABECULAR MESHWORK AND OF SCHLEMM'S CANAL: A NEW INSIGHT INTO THE REGULATION OF AQUEOUS OUTFLOW IN THE EYE

BY **Jorge A. Alvarado MD,*** Ru-Fang Yeh PhD, Linda Franse-Carman BS, George Marcellino PhD, AND Michael J. Brownstein MD

ABSTRACT

Purpose: To test the hypothesis that trabecular meshwork endothelial cells (TMEs) regulate aqueous outflow by actively releasing ligands that upon binding to Schlemm's canal endothelial cells (SCEs) increase transendothelial flow, thereby facilitating the egress of aqueous.

Methods: We tested our hypothesis by (1) activating the TMEs in vitro using a laser procedure known to increase aqueous outflow in vivo; (2) demonstrating that lasered TMEs become activated at the genome-wide level and synthesize ligands; (3) ascertaining that media conditioned by laser-activated TMEs and ligands therein increase transendothelial flow when added to SCEs; and (4) determining that ligands identified as synthesized by TMEs increase permeability when added to SCEs.

Results: We find that adding either media conditioned by lasered TMEs or ligands synthesized by TMEs to naïve control SCEs increases permeability. Adding media boiled, diluted, or conditioned by nonlasered TMEs abrogates these permeability effects. Media conditioned by either lasered TMEs or SCEs (TME-cm/SCE-cm), when added to untreated controls of each cell type, induce congruous gene expression and flow effects: TME-cm induces far more differentially expressed genes (829 in control TMEs and 1,120 in control SCEs) than does the SCE-cm (12 in control TMEs and 328 in control SCEs), and TME-cm also increases flow much more (more than 11-fold in control TMEs and more than fourfold in control SCEs) than does the SCE-cm (fivefold in control TMEs and twofold in control SCEs).

Conclusions: As postulated, the TMEs release factors that regulate SCE permeability. Derangement of this TME-driven process may play an important role in the pathogenesis of glaucoma. Ligands identified, which regulate permeability, have potential use for glaucoma therapy.

Trans Am Ophthalmol Soc 2005;103:148-163

INTRODUCTION

The conventional aqueous outflow pathway functions to facilitate the egress of aqueous from the anterior chamber of the eye into the lumen of Schlemm's canal and to prevent the reflux of blood from the venous circulation into the aqueous-filled intraocular fluid compartment.¹ The pathway is endowed with certain anatomic and cellular features that are particularly well suited to carry out these two tasks. One of these is the presence of two cellular barriers separating the venous circulation from the aqueous humor, instead of the single barrier that usually divides adjacent fluid compartments from each other elsewhere in the body. The two barriers are positioned in series so that as aqueous exits from the eye, it first encounters the trabecular meshwork endothelial cells (TMEs) that line aqueous channels, and then subsequently encounters the endothelial cells that line the lumen of Schlemm's canal (SCEs). The salient cellular feature is the presence of "giant vacuoles" in SCEs, unique organelles that form a transcellular fluid pathway.² The SCEs facilitate aqueous outflow by forming giant vacuoles only when the intraocular pressure (IOP) exceeds the episcleral venous plexus pressure. Similarly, the SCEs prevent the reflux of blood by eliminating this transcellular pathway when the episcleral venous pressure exceeds the IOP level, as occurs during intraocular surgery.² In sharp contrast to the SCEs, which are generally believed to be the site of major resistance to aqueous outflow,^{1,3} the manner in which TMEs participate in the regulation of the egress of aqueous remains poorly understood. We surmise that the TMEs also have mechanisms geared to facilitate outflow and prevent the reflux of blood, much in the manner of SCEs, but that such activities are subtle, involving a combination of processes at the molecular and cellular levels, which have yet to be identified.

Specifically, we propose that the TMEs have a relationship with the SCEs, which can be characterized by the release of ligands from TMEs into the aqueous humor. The ligands flow downstream from TMEs to bind and actively regulate the permeability properties of the SCEs. When the process mediating the interaction of TMEs and SCEs is switched on, the ligands are actively released and facilitate aqueous outflow by increasing the permeability of the SCE barrier. When the process is switched off, ligands are no longer released, forestalling the reflux of blood into the eye in some measure. Effective methods to uncover our proposed TME-to-SCE interactions can be attributed to developments from recent studies of several TME-to-TME relationships.⁴ These studies report that cytokines released by TMEs induce a wide array of effects, depending on the location of the TMEs targeted by these agents. That is, three cytokines (interleukin-1 α and 1 β and tumor necrosis factor- α [IL-1 α , IL-1 β and TNF- α]) released by TMEs

From the Departments of Ophthalmology (Dr Alvarado, Ms Franse-Carman) and Epidemiology and Biostatistics (Dr Yeh), University of California San Francisco (UCSF); OptiMedica Corporation, Santa Clara, California (Dr Marcellino); and J. Craig Venter Institute, Rockville, Maryland (Dr Brownstein). Supported by a major grant from the Thomas J. Long Foundation; the Peninsula Community Foundation; That Man May See, Inc; the Department of Ophthalmology at UCSF; Research to Prevent Blindness, Inc; Coherent Inc; Lumenis Inc; the Joan Leidy Foundation; and contributions from many generous patients of Dr Alvarado.

*Presenter.

Bold type indicates **AS** member.

located in the inner trabecular meshwork surface induce cell division and migration upon binding to TMEs located near Schwalbe's line, whereas upon binding to TMEs near the juxtacanalicular tissues, they induce the release of matrix metalloproteinases and an increase of fluid flow across extracellular matrix tissues.⁴⁻⁹

A critical step of this approach is the activation of the endothelial cells by the application of light energy using an argon laser instrument, which is known to increase aqueous outflow clinically. In the case of the argon laser, the same three cytokines are released when whole trabecular meshwork tissues are lasered in organ culture conditions.¹⁰ The argon laser has the disadvantage of drilling holes through the endothelial cells, inducing collateral thermal effects around the laser impact site, which effectively disrupt the physical integrity of endothelial monolayers after irradiation. Such a disruption makes the study of laser-induced permeability effects cumbersome. Here we introduce the use of a recently developed frequency-doubled, Q-switched, Nd:YAG laser (F-D Nd:YAG) that makes these permeability studies possible because, unlike the argon laser, the F-D Nd:YAG instrument preserves the integrity and baseline permeability properties of the endothelial monolayer immediately after irradiation. Subsequently, with a latency of several hours, there is a gradual increase in flow detectable around 12 hours, eventually peaking approximately 2 days after irradiation.

In testing our hypothesis *in vitro*, we began by applying low-fluence light energy using the F-D Nd:YAG laser to human cultured TMEs, which are then maintained in culture for a specified period of time, and allowing these cells to release putative factors into the cell-culture medium. This conditioned medium is subsequently added to untreated naïve monolayers of SCEs to determine the capacity of TMEs to modulate the permeability of SCEs. Whether the lasered TMEs become activated is determined by monitoring gene inductions at the genome-wide level (Affymetrix gene chips), verifying these inductions using mRNAs (quantitative polymerase chain reaction [Q-PCR]), and ascertaining that corresponding cytokines are synthesized (enzyme-linked immunosorbent assay [ELISA]). Those cytokines exhibiting a dose-response relationship in terms of mRNA/cytokine-expression and permeability effects are considered as candidate ligands to be added individually to monolayers of SCEs to ascertain their direct involvement in the permeability effects of SCEs. Other experiments compare treatment responses by each endothelial cell type to the laser procedure, to the addition of media conditioned by lasered TMEs, and by lasered SCEs. Results from these *in vitro* studies strongly support the concept that TMEs modulate the permeability of SCEs as advanced in our hypothesis. The "Discussion" section considers the relevance of these findings in terms of (1) the TMEs playing a prominent role in the regulation of aqueous outflow *in vivo*, (2) the mechanism of action of laser trabeculoplasty and miotics during the treatment of glaucoma patients, (3) the pathogenesis of glaucoma, and (4) potential treatment modalities using uncovered cytokines and other agents.

METHODS

This study received Institutional Review Board approval (approval number: H111-00511-22) from the University of California, San Francisco, Committee on Human Research. Informed consent was obtained from patients and tissue donors according to standard procedures.

CELL PREPARATION

Primary cultures were established by dissecting healthy human eyes to obtain explants from the trabecular meshwork containing TMEs, or from Schlemm's canal to obtain SCEs. The dissection was carried out using sterile technique; the operating microscope and methods that have been previously described in detail.^{2,11-17} We have demonstrated that *in vitro* the cultured TMEs and SCEs exhibit distinct phenotypes and possess many of the attributes displayed *in vivo* by the tissues of origin.² The primary cultures were extensively expanded and stored as frozen stocks at the fourth passage. The stocks were defrosted and cells of each type seeded separately in 10-cm culture dishes using standard media conditions (Dulbecco's modified Eagle's medium supplemented with 15% fetal calf serum, 2 μ M L-glutamine, and 50 μ g/mL of gentamicin). One week later, the nearly confluent fifth passage cells were dissociated (0.05% trypsin, 0.02% EDTA, 0.58 gm/L NaHCO₃) and transferred again (ie, sixth passage) at a concentration of 5.0×10^4 cells/cm² into 6.0- or 1.0-cm methylcellulose Millipore filter supports having 0.45- μ m pores (Millipore PIHA01250, Bedford, Massachusetts). The culture specimens were kept in a humidified 8% CO₂ incubator and fed every 48 hours until they had reached confluence (about 10 to 14 days for both cell types), when the serum concentration was reduced to 10% prior to feeding melanin particles in preparation for the laser procedure.

LASER TREATMENT

In preparation for the laser treatment, some TMEs and SCEs were fed melanin, whereas others were used as controls and remained without exposure to melanin granules. The melanin particles can act as chromophores, which are targeted by the F-D Nd:YAG laser.¹⁸⁻²¹ The presence of melanin particles was helpful in that it allowed us to apply relatively low energy levels (ie, 0.2 to 0.8 mJ/pulse) to carry out dose-response experiments, as well as to minimize the variability in the responses elicited. Melanin previously proven well tolerated by cultured cells (Sigma, St Louis, Missouri) was used to feed the TMEs and SCEs, with 3 million melanin particles per milliliter for 18 hours. The media were decanted, and the particles, which had not been ingested by the cells and thus remained free in the media, were counted by using the hemocytometer to ascertain that similar pigment loads had been taken up by each cell type. Afterwards, the cultured cells were given fresh media and returned to the standard feeding conditions for 1 week to establish that baseline permeability properties had been restored before proceeding with the laser treatment.

The F-D Nd:YAG laser used to irradiate the cultured cells emits light with a λ of 532 nm, a beam measuring 400 μ m in diameter,

and a pulse duration of ~3 ns. The laser was set to deliver ~0.8 mJ/pulse for a fluence of 600 mJ/cm², which was shown to preserve the physical integrity of the monolayer as well as the baseline permeability properties immediately after the lasering procedure. Afterwards, there was a change in permeability that occurred with a latency of several hours, progressing steadily to reach a peak ~48 hours after lasering. The TMEs/SCEs grown over 6-cm porous filter supports received 400-laser shots per preparation, and those measuring 1 cm in diameter received 25 pulses per preparation while maintained under sterile conditions. Controls consisted of preparations remaining without any laser treatment.

CONDITIONED MEDIA PREPARATION

In preliminary experiments, we determined that a period of 12 hours was sufficient for the lasered cells to reach peak conditions regarding the release of three cytokines tested (IL-1 α , IL-1 β and TNF- α). Therefore, the preparations remained in contact with the media for 12 hours after lasering to allow the media conditioning process to take place. At this time, other containers of similar size, which remained undisturbed for 12 hours, had their media decanted and replaced with media conditioned by the lasered cells of the same or the other type. The media were then allowed to remain in contact with the cell for 36 hours, and at the end of this period the hydraulic conductivity was measured in perfusion experiments in $\mu\text{L}/\text{min}/\text{mm Hg}/\text{cm}^2$. Other assays determined the gene expression profile (Affymetrix gene chips), levels of specific mRNAs (quantitative PCR), and protein synthesis and peptides released (ELISA). Controls consisted of untreated cells given media from other preparations, which had not been lasered but had received melanin, or given media that had been boiled or diluted ten times by the addition of fresh media.

CONDUCTIVITY MEASUREMENTS

The conductivity of monolayers grown over porous Millipore filter supports was determined by perfusing these cells from the apical toward the basal cell surface at a constant pressure of 4.5 mm Hg while measuring the rate of transendothelial fluid flow in $\mu\text{L}/\text{min}/\text{mm Hg}/\text{cm}^2$.^{2,15,22} The preparations are placed on a computer-driven apparatus and perfused with culture media at a transendothelial pressure of 4.5 mm Hg until stable measurements are recorded for at least 5 minutes. We measured the conductivity of filter supports containing the sixth passage cells remaining as either untreated controls, cells treated by exposure to conditioned media, or by the application of a standard number of laser pulses. Monolayer of SCEs were perfused with various cytokines to determine conductivity effects. The concentrations used were 10 ng/mL for IL-1 α and IL-1 β , 15 ng/mL for TNF- α , and 5 ng/mL for IL-8.

TOTAL RNA EXTRACTION

The various control and experimental preparations underwent total RNA extraction with Trizol reagent following the manufacturer's instructions (Invitrogen, Carlsbad, California). The preparations were washed once with PBS at room temperature, and then the cells were broken down by using 600 μL of Trizol and stirring with a rubber policeman. The lysate was withdrawn and passed through a 25-gauge syringe to break up chromosomal DNA. Adding 100 μL of chloroform to each sample and centrifuging at 12,000 rpm for 10 minutes accomplished phase separation of the tRNA. The resultant aqueous phase was transferred into a fresh container to which 600 μL of isopropyl alcohol was added prior to centrifugation for 10 minutes at 4°C to precipitate the tRNA. The tRNA precipitate was washed twice with 75% ethanol, dried briefly, and dissolved in nuclease-free water. The concentration of extracted total RNA was measured by spectrophotometric absorbance at 260 nm, and deemed acceptable when absorbance ratio at 260/280 nm was equal to or greater than 1.8.

GENE CHIP ASSAYS

Samples of sscDNA were prepared by using the NuGEN Technologies Ovation RNA amplification and Biotin Labeling system (Version 1.0) according to the manufacturer's instructions from the indicated amount of starting RNA (5 to 100 ng) as previously reported.²³ All reactions were performed in 0.2-mL strip PCR tubes in an MJ GeneWorks PTC-100 thermocycler using recommended programs. Because the seal for PCR tubes and caps tends to deteriorate with repeated use, we replaced the caps for each tube before each resealing step in the protocol. Following amplification, sscDNA product was purified using QIAquick PCR purification kits (Qiagen, Valencia, California). Samples were fragmented and end-labeled with biotin. After stopping, each reaction was concentrated in a Microcon YM-3 column to a final volume of ~20 L. The concentrated material was purified using a Centri-Sep 100-spin column (Princeton Separations, Adelphia, New Jersey).

For DNA microarrays, all samples were placed in standard Affymetrix hybridization buffer. The sample denaturation time for the sscDNA samples was reduced from 5 to 2 minutes and hybridization time increased from 16 to 20 hours as recommended by NuGEN Technologies. Arrays were stained with phycoerythrin-streptavidin according to manufacturer's recommendations.

QUANTITATIVE PCR

The concentrations of specific mRNAs were measured by using a 5' fluorogenic nuclease assay in real-time quantitative PCR on the ABI PRISM 7900 (Applied Biosystems, Foster City, California). The total RNA was extracted as described above from cultured human TMEs and SCEs, and the quality of the RNA was ascertained by using a Bioanalyzer (Agilent, Palo Alto, California). Total RNA was incubated with DNase (DNA-free, Ambion, Austin, Texas) to remove contaminating host and viral DNA. The DNase was inactivated and removed according to the manufacturer's specifications. "No reverse transcriptase" controls were performed on all samples to confirm that genomic DNA was not present. RNA was reverse transcribed into cDNA with iScript (BioRad, Hercules,

California), 300 ng in a 20- μ L volume according to manufacturer's specifications. Quantitative detection of specific nucleotide sequences was based on the fluorogenic 5' nuclease assay, as summarized by Ginzinger.²⁴ Primers and probes for the assays were obtained from Applied Biosystems "assays on demand" Taqman expression kits. Relative expression in comparison to two control genes, Cyclophilin and Gus, was calculated by using described methods.²⁵ These two control genes were chosen because they were shown to be the least variable under these experimental conditions (data not shown).

ELISA ASSAYS

Selected cytokines and chemokines released into the media were measured using ELISA. Aliquots were obtained for these assays from the 6-cm filters representing the various controls, preparations treated with exposure to media conditioned by each cell type separately, and preparations receiving a standard number of low-fluence laser pulses. The cells were disrupted by using a lyses buffer containing 1.0% NP-40, 150 mM NaCl, and 50 mM of tris at pH 8.0. A complement cocktail of protease inhibitors was added containing PMSF 1.0 mM, 1 μ mol/L each of pepstatin and leupeptin, and 0.3 μ mol/L of aprotinin. The preparations were placed on an agitator at room temperature for 1 hour, scraped into Eppendorf tubes, and sonicated for 30 seconds. The supernatant was separated from the cellular debris by centrifugation at 2,000 rpm for 20 minutes, collected, and transferred to cryovials with one portion of the sample stored in liquid nitrogen for later analysis and the other assayed immediately.

The assay began by adding samples to the micro plate wells containing the specific antibody adherent and immobilized to its surface. After the cytokines became bound to their specific antibodies, unbound substances were removed by vigorous buffer washing, followed by the addition of enzyme-linked polyclonal antibody to each well. A substrate solution was then added to each well and the intensity of the resultant color reaction was measured by using a micro plate spectrophotometer reader set to the proper wavelength. Optical density values from duplicate-control standards and quadruplicate experimental samples were averaged separately. The obtained average zero-standard optical density value was subtracted from that of the standard and experimental sample readings. A standard curve was constructed by plotting the mean absorbance for each standard on the y-axis, and the values of the samples were plotted on the x-axis. A best-fit line was plotted using regression analysis, and the optical density measurements were converted to picograms per milliliter values.

STATISTICAL ANALYSIS FOR ARRAY DATA

The raw image data were analyzed by using GeneChip Expression Analysis Software (Affymetrix, or Affy) to extract perfect match and mismatch values, to which we applied the Robust Multiarray Average (RMA) algorithm^{26,27} implemented in the Bioconductor/Affy package²⁸ under the free statistical computing environment R (<http://www.r-project.org>) to background-correct, quantile-normalize, and summarize values of 11 probe pairs for each gene (probe set) on each chip. This results in a 54,675 \times 32 matrix of logarithm-based 2 of gene expression measures, where columns correspond to different gene chips and rows correspond to the different genes (probe sets). For a typical gene (probe set), we have four replicate expression measures (from four chips) for each of the eight conditions: TME control (TC), TME treated by laser (TL), TME treated by TME-conditioned media (TT), TME treated by SCE-conditioned media (TS), SCE control (SC), SCE treated by laser (SL), SCE treated by TME-conditioned media (ST), and SCE treated by SCE-conditioned media (SS).

IDENTIFICATION OF DIFFERENTIALLY EXPRESSED GENES

The ratio-intensity plot provides a graphic method to identify and visualize differentially expressed (DE) genes. For example, to compare samples TL and TC, we computed the average differences ("fold" change in log-based 2), $M_{TL \text{ vs } TC}$, between the two cell types $M = M_{TL} - M_{TC}$. Genes with corresponding extreme $M_{TL \text{ vs } TC}$ values represent potential marker genes activated by laser treatment in TMEs. The overall expression level for a particular gene is conveniently measured by the quantity A , the average of log intensities across all the chips in the experiment. Similar calculations were made for each of the treatment conditions against their baseline controls (TL vs TC; TT vs TC; TS vs TC; SL vs SC; ST vs SC; SS vs SC). The M provides a ranking of genes corresponding to the strength of evidence of differential expression. In addition, we also computed the moderated t statistics and accompanying P values²⁹ to assess the statistical significance of the "-fold" changes for each gene. We then generated a candidate list of the number of DE genes with a 10% false discovery rate and greater than twofold change between groups. The functions used in these procedures are in the limma library of the R/Bioconductor software package.

DIFFERENTIALLY EXPRESSED GENES BY FUNCTIONS

To investigate further the difference between TME and SCE cell markers, we compared the functional composition of probe sets differentially expressed by the three treatment categories compared with controls for each cell type (i.e., eight categories). We mapped each probe set to a predefined functional group according to the Gene Ontology (GO) annotation database (<http://www.geneontology.org>) and compared the number of genes belonging to each functional group. In addition, we searched for overrepresented and underrepresented (FDR-adjusted P value $< .05$) GO categories in the various experimental and control conditions using Gostat, which calculates a Fisher's exact test P value for each GO category.

RESULTS

ACTIVATION OF TMES AND SCES

We assess the cell activation process in TMEs and SCEs by determining the number of DE genes at the genome-wide level in treated compared with untreated control preparations. Figures 1 and 2 are log-based 2 ratio-intensity MA plots, where the quantity A represents the average of log intensities across all the chips in the experiment, and M provides a ranking of genes corresponding to the strength of evidence of differential expression (see “Methods” section). In Figures 1 and 2, red and green dots represent, respectively, up- and down-regulated genes exhibiting a twofold or greater increased expression. Below each graph, the total number of corresponding DE genes is indicated, which in panel A of Figure 1 amounts to 1,570 DE genes by lasered TMEs.

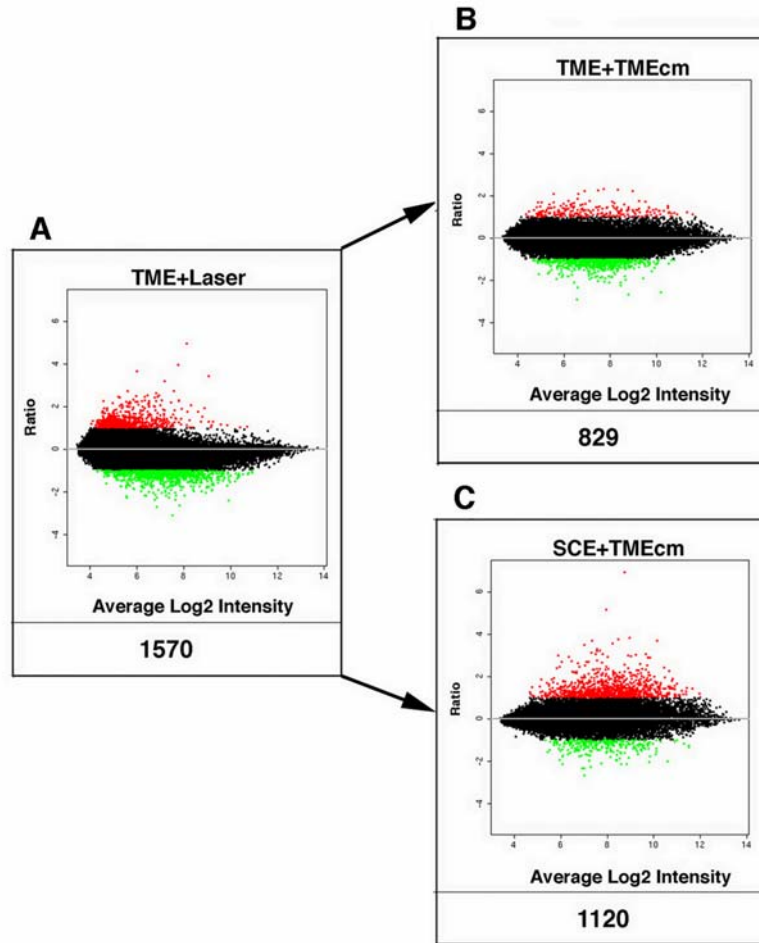


FIGURE 1

Gene expression in trabecular meshwork endothelial cells (TMEs). Log-based 2 ratio-intensity scatterplot comparing the profile of genes expressed by TMEs treated by the application of short-pulse green light delivered by a frequency-doubled Nd:YAG laser instrument (A) and by the addition of media conditioned by the lasered TMEs when added to naïve TMEs (B) or to naïve SCEs (C). Each dot represents the mean intensity log-ratio (base 2) versus the average log-intensity of a single gene based on four replicas (ie, one chip for each of four samples), with each replicate containing 11 probes per gene, using approximately 47,000 transcripts from 38,500 well-characterized genes. Red and green dots indicate up- and down-regulated genes demonstrating a twofold or greater differentially expressed (DE) ratio; the total number of DE genes for each category is indicated below each graph.

This robust laser-treatment response represents the greatest induction of DE genes observed, a finding that strongly supports the notion that TMEs are activated by treatment with the F-D Nd:YAG laser. Panel B depicts the profile of DE genes in naïve untreated control TMEs exposed to media conditioned by the laser-activated TMEs (i.e., TME-cm) showing that 829 genes are differentially expressed, which is the third most intense gene response measured. Panel C shows the response of naïve SCEs exposed to medium

conditioned by the laser-activated TMEs. The media activation process is very intense, resulting in the induction of 1,120 DE genes in SCEs, representing the second most intense response observed. Thus, the three preparations involving lasered TMEs, or naïve TMEs and SCEs exposed to the TME-cm, yield the three top responses in terms of DE genes. Further, treatment by addition of conditioned media was nearly as effective as the laser treatment itself.

Figure 2 is a similar log-based 2 ratio-intensity scatter plot as in Figure 1 showing the responses in lasered SCEs (A), or preparations containing naïve SCEs exposed to medium conditioned by the lasered SCEs (B) and naïve TMEs (C).

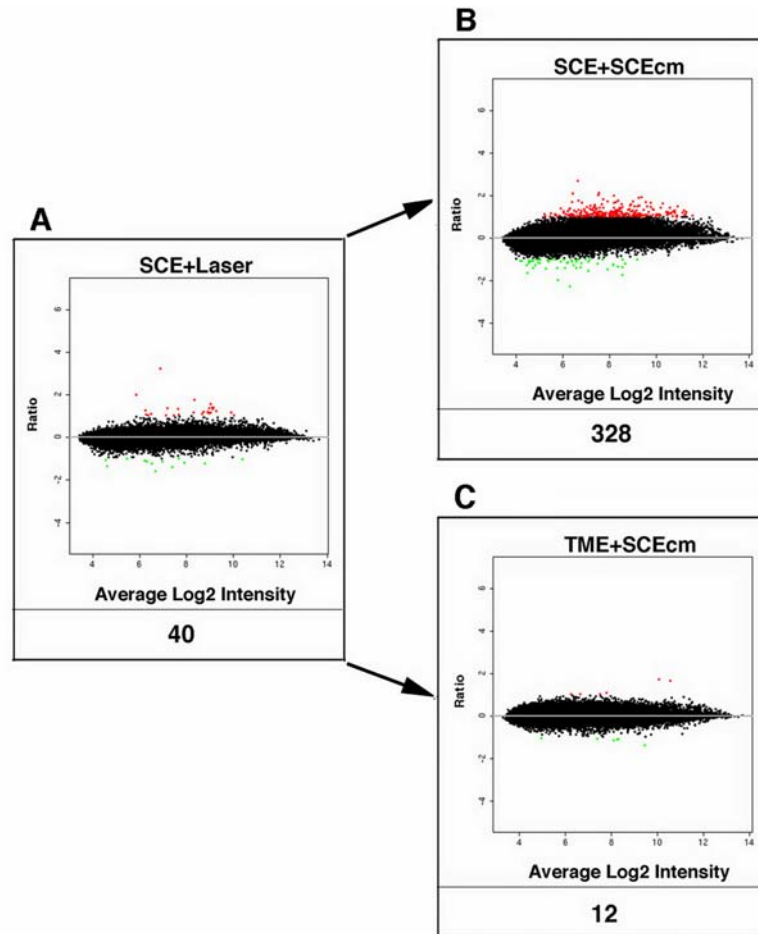


FIGURE 2

Gene expression in Schlemm's canal endothelial cells (SCEs). Log-based 2 ratio-intensity scatterplot showing profiles of differentially expressed DE-genes in SCEs after the laser procedure (A) and by the addition of SCE-cm to naïve SCEs (B) or to naïve trabecular meshwork endothelial cells (TMEs) (C).

The laser procedure, which induces the most DE genes when applied to TMEs (1,570), is markedly less effective in the case of lasered SCEs, inducing only 40 DE genes. Despite the fact that the laser procedure activates only 40 genes in SCEs, medium conditioned by these laser-activated SCEs is actually quite effective as it induces an eightfold increase in the number of DE genes when added to control SCEs (ie, 328/40) (B). The addition of the medium conditioned by the laser-activated SCEs to naïve TMEs yields the least effective response with the induction of only 12 DE genes (C). Media exposure effects appear to vary markedly, depending on the type of cell conditioning the medium and the type of cell receiving the medium treatment. In the case of TMEs (Figures 1 and 2), medium conditioned by the lasered trabecular cells (which are maximally activated) is quite effective in activating both naïve TMEs and SCEs. However, in the case of SCEs (Figure 2), medium conditioned by the lasered Schlemm's canal endothelial cells (which are minimally activated) is most ineffective in activating TMEs but quite effective in activating SCEs. Therefore, it seems that media effects are not only cell-specific but also proceed in both directions, yielding either intense or minimally effective responses, depending on the cell type treated and the conditioned medium applied.

Table 1 shows a list of DE genes with a 10% false discovery rate and greater than twofold change between functional groups as indicated. The responses obtained when applying different cutoff criteria are shown in Table 1. The values used in Figures 1 and 2 correspond with those measured when a twofold cutoff is applied. Use of a fourfold cutoff or a *P* value of .01, separately or together, results in a smaller number of DE genes detected. It can be seen that for the TME category, lasered TMEs consistently exhibit a

TABLE 1. DIFFERENTIALLY EXPRESSED (DE) GENES IN VARIOUS TREATMENT CATEGORIES*

P VALUE CUTOFF										
.01										
“-FOLD” CHANGE CUTOFF										
2			4			4				
DE GENES	TOTAL	UP	DOWN	TOTAL	UP	DOWN	TOTAL	UP	DOWN	
TL/TC	1,570	641	929	68	45	23	67	44	23	
TcmT/TC	829	220	609	17	7	10	14	4	10	
TcmS/TC	12	6	6	0	0	0	0	0	0	
SL/SC	40	27	13	1	1	0	1	1	0	
ScmT/SC	1,120	855	265	97	87	10	91	82	9	
ScmS/SC	328	275	53	5	4	1	4	3	1	

*Number of DE genes is shown according to the treatment category, the “-fold” change, and the *P* value cutoff. The first three rows under “DE Genes” pertain to trabecular meshwork endothelial cells (TMEs) and the last three rows represent Schlemm’s canal endothelial cells (SCEs). Note that the count of DE genes declines as more stringent criteria are applied. In general, the trends are maintained regardless of the cutoff criteria used. Note that the total number of genes considered for each condition is approximately 28,000.

greater number of DE genes than TME-cm/TMEs, which in turn show a greater number of DE genes than SCE-cm/TMEs. The SCE category is similarly consistent regardless of cutoff criteria used, with TME-cm/SCE having a greater number of DE genes, followed by SCE-cm/SCE, and then lasered SCEs.

CONDUCTIVITY EFFECTS

In panel A of Figure 3, we show the conductivities measured in TMEs treated by laser, or by exposure to media-conditioned lasered cells of each type compared with untreated controls (red bars). Alongside we show the responses in SCEs (green bars) in control and similarly treated preparations. In panel B of Figure 3, we show the treatment responses when corrected for baseline differences and expressed as a “-fold” change. The conductivity responses vary as a function of the treatment applied as well as the cell type treated (Figure 3B).

In general, comparing the six responses plotted demonstrates that the TME responses (red bars) are higher than those in SCEs (green bars). This disparity in conductivity responses seems to be well correlated with the gene expression data in Figures 1 and 2 showing that the laser effects are markedly disproportionate, with the TMEs undergoing a much greater response to the laser treatment compared with the SCE (1,570 versus 40 DE genes). The TME-cm is also much more effective in inducing the differential expression of genes when added to TMEs as well as SCEs, compared with the effects of medium conditioned by laser-activated SCEs upon TMEs or their own cell type. Regarding media effects, the TME-cm induces an increase in conductivity that is maximal for both TMEs (second red bar) and SCEs (second green bar). These differences are mirrored as well in the gene expression data, because the TME-cm is also potent in inducing DE genes when applied to naïve TMEs and SCEs (ie, 829 and 1,120 respectively).

The relationships between the gene expression and conductivity are incongruous in some instances. For example, the conductivity responses of the laser procedure in both TMEs and SCEs are exactly the same, amounting to a threefold increase in conductivity in each case (Figure 3B). However, the gene expression data are most disparate involving the induction of 1,570 DE genes for TMEs but only 40 for the SCEs. Similarly, the SCE-cm, which induces only 12 DE genes when added to TMEs, induces the second highest change in conductivity (Figure 3B). These discrepancies suggest that only a small proportion of DE genes are actually involved in mediating the measured conductivity effects.

Analyzing the conductivity effects of the laser procedure in Figure 3B, it is apparent that some effects are related to “systematic” differences in the preparations compared. That is, for the TMEs, the laser treatment induces a much smaller increase in conductivity (ie, threefold change) than exposure to the TME-cm, which induces almost a fourfold greater conductivity increase that amounts to an 11-fold increase. A similar, albeit less pronounced, relationship is apparent for the SCEs (compare first and second green bars).

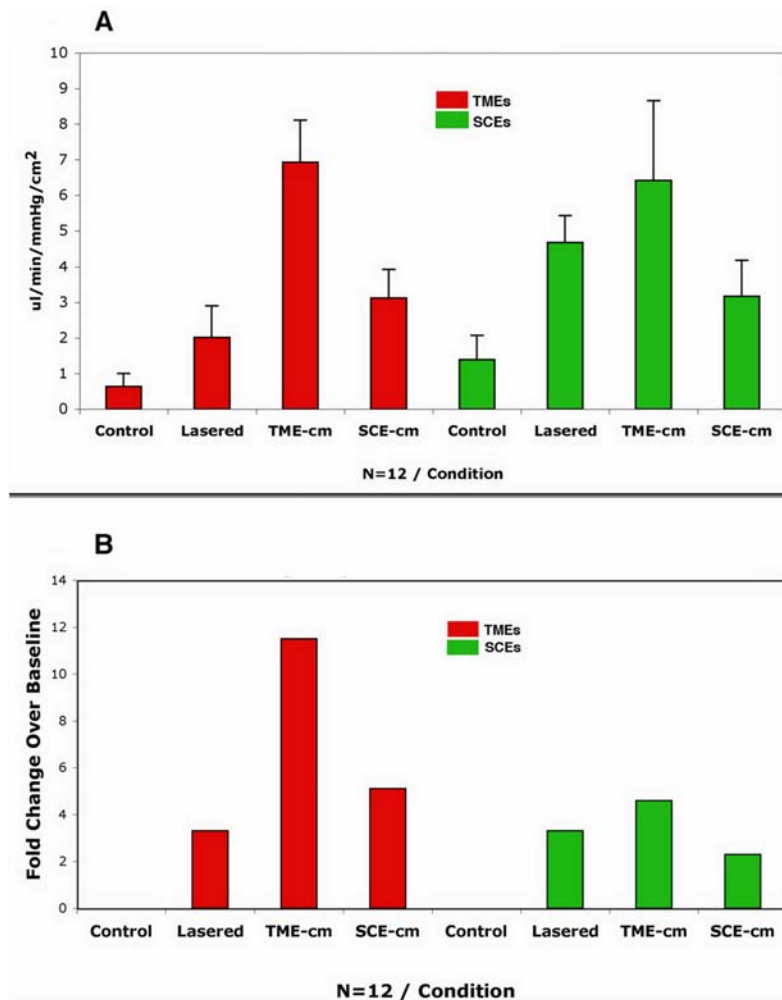


FIGURE 3

Conductivity responses measured in $\mu\text{L}/\text{min}/\text{mmHg}/\text{cm}^2$. Bars represent the mean and the standard deviation in panel A for monolayers of trabecular meshwork endothelial cells (TMEs) and Schlemm’s canal endothelial cells (SCEs) in both controls and treated preparations as indicated. In panel B the treatment responses are depicted, adjusting for differences in baseline as a “-fold” change. Note that in all cases, the responses are robust, amounting to increases of over 11-fold in the case of the TME-cm, the highest response, and 200% in the case of naïve SCEs treated with SCE-cm, the smallest response.

We suspect that such disparate responses mirror the fact that each of these two preparations has a different cell composition. The lasered preparations include two cell types: (1) cells impacted by the laser beam and (2) cells that remain untouched by the laser treatment. Assuming that only the nonlasered cells are capable of responding fully, then the lasered preparations have a smaller proportion of cells capable of mounting a full response to factors released in the media, whereas preparations treated with media exposure have 100% responsive cells. Thus, media-treated preparations would be expected to yield responses having a conductivity of greater magnitude than laser-treated preparations.

CONTROLS

Several controls, as shown in Figure 4, were used to ascertain that the conditioned media effects were mediated by factors released into the media by the laser-activated TMEs. The first control in Figure 4 requires adding media from naïve untreated TMEs to other naïve TMEs. The second control requires diluting the media conditioned by laser-activated TMEs fivefold by the addition of plain cell culture media. In the third control, any factors present in the media conditioned by laser-activated TMEs are denatured and inactivated by boiling these media for 5 minutes. Results demonstrate that diluting and boiling effectively inactivate the media because these two conditions yield similar responses as adding media from naïve TMEs (compare first with second and third bars). In contrast, media from laser-activated TMEs (red bar) induce a twofold increase in conductivity.

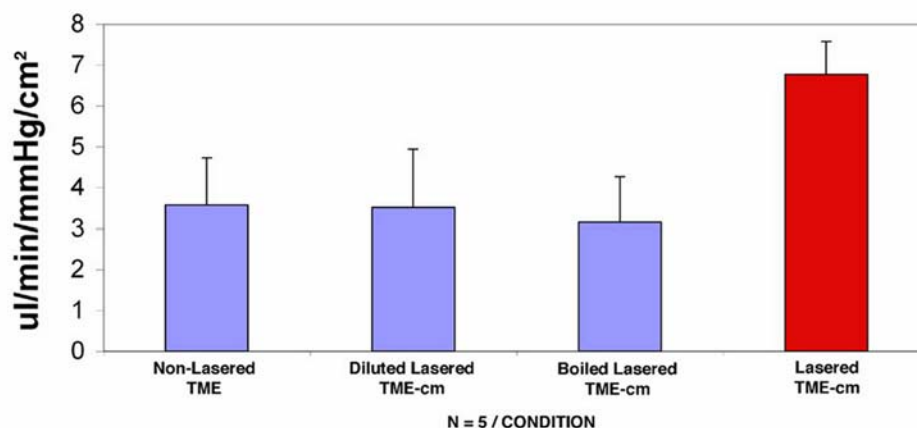


FIGURE 4

Conductivity responses in preparations exposed to inactivated media compared with intact medium. Conductivity responses measured in $\mu\text{L}/\text{min}/\text{mm Hg}/\text{cm}^2$ showing the mean and standard deviation in controls (blue bars) and in trabecular meshwork endothelial cells (TMEs) treated by the addition of media conditioned by laser-activated TMEs (red bar). Adding media from naïve TMEs, or from laser-activated TMEs that had been inactivated by dilution or boiling, effectively abrogated the increase in conductivity as observed when media conditioned by lasered TMEs was added (red bar).

CORRELATION OF GENE EXPRESSION PROFILES, SPECIFIC MRNA LEVELS, AND CYTOKINE SECRETION WITH CONDUCTIVITY

Figure 5 displays the cDNA transcript and peptide responses for the chemokine IL-8 in the same eight conditions represented in the conductivity experiments in Figure 3A. Table 2 gives the nominal P values for two-sample t tests among the eight conditions tested. In Figure 5, panel A, the cDNA expression responses are shown in terms of the signal intensity detected for IL-8 in TMEs (red bars) and SCEs (green bars). The TMEs responses shown in this panel are more intense than those elicited in SCEs, regardless of experimental condition. For the TMEs, only the lasered preparation exhibits a significantly different response from its control ($P = .0026$, see Table 2, Affy cell); for the SCEs, the preparation treated with the TME-cm differs most significantly from its control ($P < .0001$). Noting the occurrence of these two significant findings motivated us to proceed and determine more accurately mRNA expression using q-PCR, which is shown in panel B. Again the TMEs yield greater responses across the board compared with SCEs. Within the TMEs (red bars) and as shown in Table 2, whereas the three-treatment preparations are different from controls, the significance levels are borderline except for the SCE-cm category ($P = .0048$). In the case of the SCEs (green bars), the TME-cm and SCE-cm treated preparations have a significant increase in mRNA expression from its control ($P = .0153$ and $.0026$, respectively).

It should be noted that the relative height of the bars for the three experimental conditions (ie, excluding control responses) for the TMEs appears to be the same in panels A and B, and similarly for the SCEs. That is, for the TMEs, the lasered TMEs in both panels have the highest columns, the SCE-cm preparations are the next highest, followed by the TME-cm. In the case of the SCEs, the TME-cm is the highest column, with the height of the remaining indistinguishable from each other in both panels A and B. In fact, the Q-PCR assays both support and extend the gene expression results. Specifically, there appears to be a more pronounced activation for the TMEs than SCEs, as well as distinct treatment responses. In panel C, we plot the responses for the preparations in terms of the synthesis of the protein IL-8 measured using ELISA. These data yield responses that show clear differences among most categories compared. In particular, we note that TME preparations treated with either the laser procedure or the addition of TME-cm display marked increases in IL-8 levels relative to controls. However, the response of TMEs exposed to the SCE-cm is virtually identical and not different from controls statistically. For the SCEs, the three treatments yield increases in IL-8 synthesis relative to controls, which are highly significant (see Table 2).

These ELISA findings in panel C are compared in panel D with the corresponding conductivity results, as depicted in Figure 3A. The conductivity responses are highly significant in all the preparations compared with controls ($P < .0001$). Inspection of panels C and D shows that in seven of eight conditions (or five of six treatment conditions), similar responses are measured by both assays.

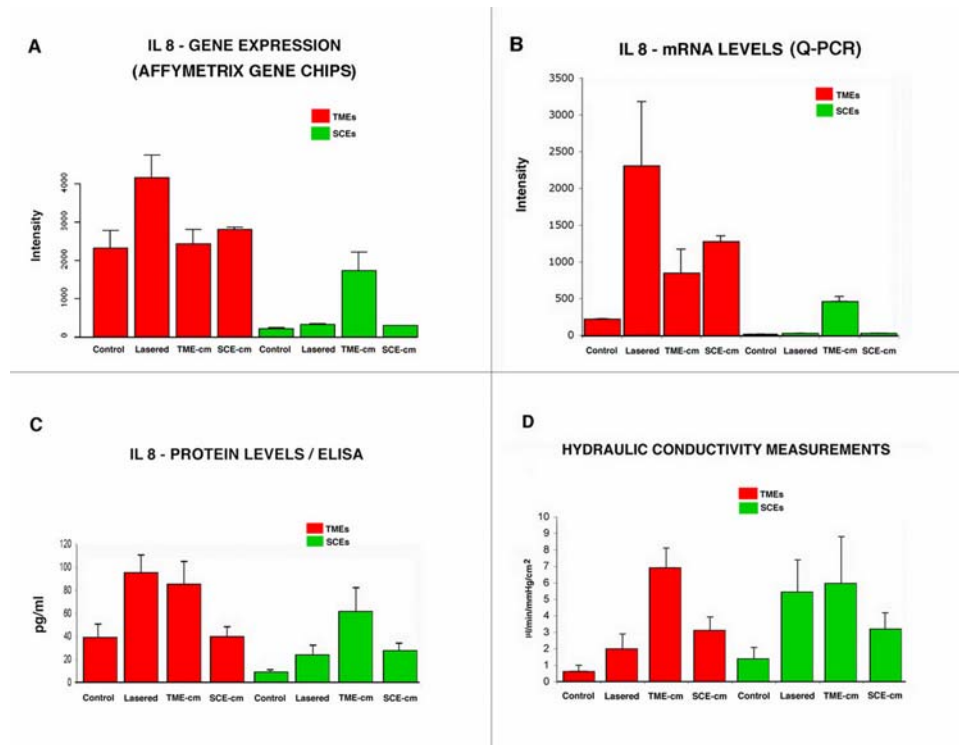


FIGURE 5

Correlation of cDNA, mRNA, and cytokine expression with conductivity. Intensity plot depicting the responses measured (mean and standard deviation) in the eight experimental and control preparations. mRNA level using Affymetrix gene chips (A), quantitative polymerase chain reaction (PCR) measured using quantitative PCR (Q-PCR) (B), at the protein level measured using enzyme-linked immunosorbent assay (ELISA) (C). These responses are correlated with those measured in conductivity assays (D). The mRNA responses are measured as the mean intensity log-ratio (base 2). The ELISA measurements are expressed in picograms/mL, and the conductivity studies units in $\mu\text{L}/\text{min}/\text{mm Hg}/\text{cm}^2$.

However, there are notable differences that we attribute to the fact that in the experiments for panel C, we are simply measuring levels for a given cytokine, whereas in panel D, we are actually measuring the responses to many such factors. These responses are likely influenced by the profile and affinity of receptors expressed by each cell type and other interactions. In general, Figure 4 shows that at the mRNA and protein levels, the responses observed in the TMEs are greater than those in the SCEs. Again, these findings mirror those observed for the gene induction and conductivity studies previously described (Figures 1, 2, and 3). The synthesis of IL-8 by TMEs (and SCEs) is consistent with IL-8 mediating, along with other factors, the conductivity effects detected in our experiments.

CYTOKINE SYNTHESIS BY LASER-ACTIVATED TMEs

The assays shown in Figure 5 demonstrate that the TMEs are activated at the gene level to express the appropriate transcripts for a given cytokine, signals that lead to the synthesis of the corresponding mRNAs and, ultimately, to the synthesis and release of the chemokine IL-8. Importantly, these responses occur in a congruous manner to the induction of conductivity increases in multiple conditions tested. We decided to seek further evidence by using ELISA in support of the synthesis of the cytokines IL-1 α , IL-1 β , and TNF- α . As mentioned in the “Introduction,” these three cytokines are released by TMEs after the application of light energy using an argon laser. However, it is unknown whether the F-D Nd:YAG is similar to the argon laser in terms of the induction of these cytokines.

Figure 6 is a plot comparing the synthesis and release of IL-1 α and IL-1 β by TMEs receiving a standard number of laser shots at a setting of 1 mJ/pulse delivered using the F-D Nd:YAG laser. Whereas the responses measured are statistically significant ($P < .01$), the quantity of IL-1 α released (~30%) in picograms/mL is small compared with the greater than twofold change measured for IL-1 β . Figure 7 is a graph of the dose-response relationship between the application of the standard number of laser shots using the F-D Nd:YAG laser at increasing energy levels, from 0.1 to 1.0 mJ. There is a progressive increase in the quantity of TNF- α released as a function of the laser energy applied. Thus, we conclude that the F-D Nd:YAG laser induces the same three cytokines, which are released by these cells when treated with the argon laser.

TABLE 2. COMPARISON OF P VALUES FOR EACH EXPERIMENTAL CONDITION AND ITS CONTROL*

METHOD†	TMES‡			SCES§		
	LASERED	TME-CM	SCE-CM	LASERED	TME-CM	SCE-CM
Affy	.0026	NS	NS	.0053	<.0001	.016
qPCR	.0318	NS	.0048	NS	.0153	.0026
ELISA	.0033	.0092	NS	.0035	.0001	.0009

NS = not significant.

*Entries are the *P* values obtained for the comparisons between each experimental condition and its respective control. The *P* values are obtained from two sample *t* tests.

†Methods used to measure the expression IL-8: Affymetrix chips (Affy), quantitative PCR measurements for mRNA (qPCR), and ELISA for the IL-8 protein.

‡*P* values for the three treatments applied to TMEs: “lasered” TMEs, those treated with “TME-cm,” and those exposed to “SCE-cm.”

§*P* values of the same three conditions for SCEs compared with control SCEs.

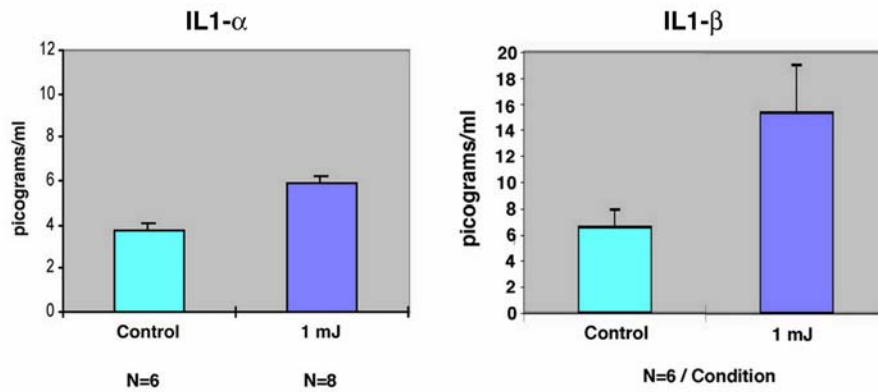


FIGURE 6

Induction of two cytokines by laser-activated trabecular meshwork endothelial cells (TMEs). Plot of the responses elicited by delivering 25 shots of 1 mJ in energy per sample in treated (n = 8) and control (n = 6) TME preparations expressed in picograms/mL. Mean and standard deviation plotted.

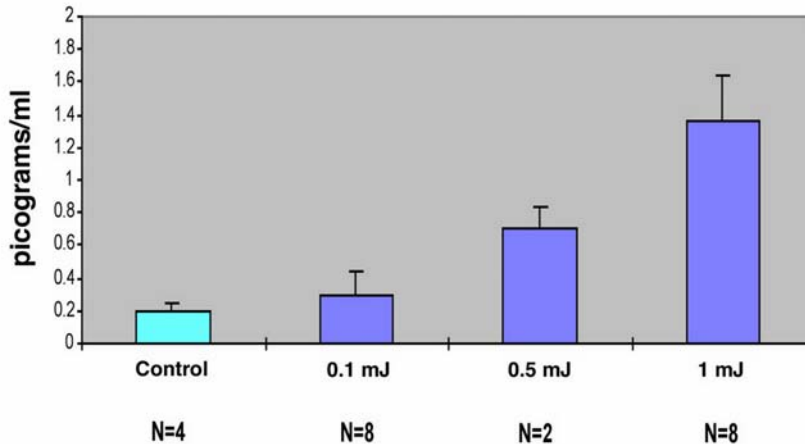


FIGURE 7

Laser energy versus tumor necrosis factor-α (TNF-α) release in trabecular meshwork endothelial cells: a dose-response effect. A dose-response effect is shown for the release of TNF-α as a function of the application of a standard number of laser shots of increasing energy as indicated. There is nearly an eightfold increase in the picograms/mL measured when using laser shots of 1 mJ in energy compared with untreated controls. Mean and standard deviation plotted.

SCES CONDUCTIVITY RESPONSE WITH ADDITION OF FOUR CYTOKINES

The four cytokines, synthesized and released into the media by TMEs, are added to monolayers of naïve SCEs while the monolayer conductivity is monitored, yielding the responses shown in Figure 8. Here the SCE-conductivity measured is plotted as a function of the type of cytokine added. At the concentrations administered for each cytokine, there is a response detected for the four factors tested. Without a dose-response curve, it is not possible to compare the potency of each agent. However, inspection of this graph shows that the four factors induce substantial increases in the SCE conductivity. These data support the concept that the conductivity effects induced by the TME-cm, when added to SCEs, are likely mediated by media-borne factors as postulated in our hypothesis.

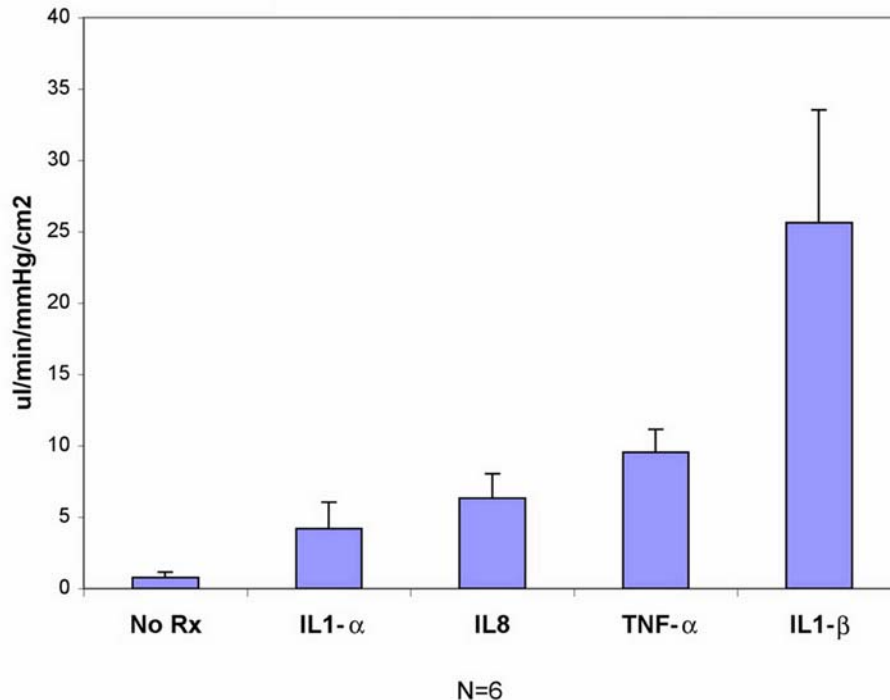


FIGURE 8

Schlemm's canal endothelial cells (SCEs) conductivity responses after the addition of indicated cytokines. Plot showing changes in conductivity induced by the direct addition to SCE monolayers of 10 ng of IL-1 α , 5 ng of IL-8, 15 ng of tumor necrosis factor- α (TNF- α), and 10 ng of IL-1 β . Mean and standard deviation are shown.

DISCUSSION

We have tested the hypothesis, *in vitro*, that the TMEs release factors into the media, and that these factors upon binding to SCEs increase the permeability of the cell barrier formed by SCEs. If the same mechanism is operative *in vivo*, by implication, increasing transendothelial fluid flow across the SCE barrier is tantamount to facilitating aqueous outflow, as these cells form the last barrier crossed by this fluid upon exiting from the eye. The validity of our hypothesis is strongly supported by the evidence provided in our studies. The TMEs, which are activated by using a laser procedure, are capable of releasing a large number of factors into the media. When aliquots of these factors are collected from the medium conditioned by the TMEs and added to SCEs, the putative factors activate the SCEs. That is, the SCEs exposed to this medium respond by producing many DE genes. Moreover, as predicted, the addition of media conditioned by the laser-activated TMEs to monolayers of untreated SCEs results in a 400% increase in SCE conductivity. The role of media factors is supported by control studies showing that boiling, diluting, or using medium from untreated TMEs abrogates the TME medium effects on SCE permeability. Finally, in two sets of experiments, we directly addressed the issue of the involvement of media-borne molecular factors released by TMEs. In one set of experiments, we demonstrated that the TMEs do synthesize and release IL-8 by demonstrating that its gene is up-regulated and that the corresponding mRNAs undergo a congruous induction, which results in the synthesis of the corresponding IL-8 protein. The second set of experiments demonstrates, using ELISA, that three other cytokines are released into the media by TMEs and, most important, when each of the four candidate cytokines are added individually to SCEs, the conductivity increases in agreement with our hypothesis.

An unexpected discovery is that the responses to the laser treatment are cell-specific, because lasering TMEs yields the differential expression of 1,570 genes compared with lasering SCEs, which yields only 40 DE genes. These differential gene responses are correlated with the potency effects of medium conditioned by each cell type. Medium conditioned by the highly laser-activated TMEs induces correspondingly large responses when added to either untreated TMEs or SCEs, generating 829 and 1,120 DE genes, respectively, for a total of 1,949. On the other hand, medium conditioned by the weakly laser-activated SCEs induces congruous small responses when added to either SCEs or TMEs, producing 328 and 12 DE genes, respectively, for a total of 340. Thus, there is at least a 500% greater induction of DE genes by TME-conditioned medium compared with SCE-conditioned medium (ie, 1,949 versus 340 DE genes). These gene differences are reflected as well in the conductivity increases induced by each cell type. Medium conditioned by the lasered TMEs induces a 200% greater increase in conductivity when added to TMEs and SCEs, compared with medium conditioned by the lasered SCEs when added to the same two cell types.

Another important finding is that the cell-to-cell interactions proceed in both directions, involving TME-to-SCE and SCE-to-TME relationships, as well as mutual exchanges involving TME-to-TME and SCE-to-SCE associations. In the case of some of these interactions, the conductivity effects are not strictly related to the differential induction of genes. For instance, the lasered SCEs undergo the DE of only 40 genes, but medium conditioned by these lasered SCEs when added to naïve SCEs induces 320 genes, a response that represents an eightfold increment. To explain these seemingly disparate effects, we propose that SCEs have a receptor profile and binding affinity that favors factors released by lasered SCEs. Other responses proceed in the opposite direction, such as those when medium conditioned by lasered SCEs is added to naïve TMEs (12 DE genes). The SCEs undergo the induction of 320 genes when exposed to SCE-cm, which suggests that this medium probably contains a large complement of factors. Yet, when the SCE-cm is added to naïve TMEs, these cells respond by undergoing the DE of only 12 genes, the smallest response detected. In this circumstance, we conjecture that the binding affinity and receptor profile of TMEs is particularly insensitive to the effect of factors released by the SCEs. In future experiments, we will control for differences in cell activation by manipulating the content of chromophores given, as well as the amount of laser irradiation delivered to each cell type, so that the desired response intensity is achieved. Understanding these differences in "sensitivity" is an important consideration in choosing factors to induce conductivity increases affecting one cell type in preference to the other for the potential treatment of glaucoma.

The finding that cytokines released by TMEs regulate the permeability of the SCE barrier is novel and to our knowledge has not been previously proposed. How this TME mechanism contributes to the two functions of the trabecular meshwork to facilitate aqueous outflow and prevent the reflux of blood is not readily apparent. The requirements of such a mechanism are highlighted when one considers how the SCEs help the trabecular meshwork carry out both of these functions. Here we are referring to the formation of giant vacuoles by the SCEs. When the IOP level exceeds the episcleral venous pressure, the pressure along the basal cell surface exceeds that in the apical surface of the SCEs and provides the driving force to induce the formation of giant vacuoles. By providing the SCE barrier with an accessory outflow route, these vacuoles in turn promote the more rapid egress of aqueous. When the episcleral venous pressure exceeds the IOP, the pressure is now higher along the apical than it is along the basal cell surface, eliminating the driving force that induces the formation of giant vacuoles. Thus, giant vacuoles are no longer formed, and the barrier becomes more resistant, as would be required to prevent the reflux of blood. Measurements of the conductivity of monolayers of cultured human SCEs *in vitro* yield data that are consistent with these concepts. For instance, when perfused with fluid flowing in the same direction as followed when aqueous exits from the eye (ie, outflow direction), the conductivity of the SCEs measures 5.23 $\mu\text{L}/\text{min}/\text{mm Hg}/\text{cm}^2$, as the endothelium behaves as a leaky monolayer that can easily promote the outflow of aqueous. When the SCE monolayer is perfused in the opposite, or reflux, direction, the conductivity measures 0.66 $\mu\text{L}/\text{min}/\text{mm Hg}/\text{cm}^2$, or eight times more resistant. Such a resistance would be required to prevent, to some extent, the reflux of blood.² Therefore, these considerations help us understand how, by linking the giant vacuole formation process with that of the relationship between the IOP and the venous pressure in the lumen of Schlemm's canal, the SCEs function to assist the trabecular meshwork in carrying out its dual functions of facilitating aqueous outflow and preventing the reflux of blood.

We now use these concepts to propose that a mechanism exists for the TMEs that is essentially similar to that described for the SCEs. The trabecular meshwork and the lining TMEs, as well as Schlemm's canal and the lining SCEs, undergo deformation and stretching with changes in intraocular pressure.³⁰ Moreover, stretching the TMEs by mechanical means or by increasing the intraocular pressure elicits a wide variety of important biochemical responses.³¹⁻³⁴ Assuming that the TMEs have stretch receptors, when the IOP is greater than the venous pressure, the increased tension makes the trabecular beams and cords taut, thus triggering the stretch receptors to activate the TMEs to release vasoactive factors that then will increase flow across the SCEs. When the IOP is less than the venous pressure, the beams and cords become flaccid, resulting in the opposite response, which should increase the resistance presented by the SCEs so as to resist the reflux of blood. If such a tension-sensitive mechanism does in fact exist, it is likely that miotics, like pilocarpine, by inducing the contraction of the ciliary muscle and increasing the tension along the trabecular meshwork beams and cords, could also activate the stretch receptor to turn on the TMEs. These cells, under the influence of the miotic-mediated increase in tension, would then release the factors required to increase the SCE conductivity, and thus the egress of aqueous. We propose that the mechanical effects generating tension and biologic mechanisms releasing vasoactive factors work together. These interactions account for the action of miotics during glaucoma therapy, instead of being due to strictly mechanical effects as traditionally credited for the action of this drug.³⁵ Importantly, the validity of this theory can be readily tested using the gene activation approaches described in the present paper along with the use of TMEs grown over stretchable silicone sheets.

In primary open-angle glaucoma (POAG), the population of trabecular meshwork endothelial cells is markedly decreased compared with that of age-matched healthy subjects.³⁶⁻⁴⁰ This progressive decline in cell density results in the loss of 0.58% of the

total number of cells per year and is most pronounced in the inner layers of the filtration zone of the trabecular meshwork. The inner trabecular cells, which are the first encountered by aqueous humor, may be prone to injury by free oxygen radicals carried in this fluid.³⁹ When we first noticed the loss of TMEs in POAG, it was difficult to comprehend how this cell loss could have a negative impact on the facility of aqueous outflow and the pathogenesis of glaucoma,³⁶ particularly in view of the generally held concept that the greatest resistance to aqueous outflow is presented by the SCEs.³ Recently, sophisticated assays have been carried out which demonstrate that there is extensive oxidative DNA damage involving the trabecular cells of patients with POAG, affecting the filtration zone and the inner trabecular meshwork layers.⁴¹ Additionally, we are interested in understanding the particular mechanisms involved in the loss of trabecular meshwork cells. Other studies report that incorporating a particular type of myocilin mutant known to be present in vivo in certain types of open-angle glaucoma into TMEs in vitro (ie, Pro370Leu) actually results in what is referred to as “killing” of the cultured human TMEs. The TMEs’ demise is due to misfolding, aggregation, and buildup of this protein in the endoplasmic reticulum of the trabecular cells.⁴² Whether due to oxidative DNA damage or the abnormal processing of protein folding (ie, proteomics) by the TMEs in POAG, there is increasing evidence suggesting the involvement of several mechanisms whereby the normal population of trabecular meshwork cells is affected by dysfunction and death. In view of the present study, it is now becoming increasingly clear how such a loss of trabecular meshwork cells, by reducing the quantity of cytokines released by a diminished population of TMEs, could have a negative impact on the homeostasis of aqueous outflow. The reduced load of cytokines and other factors may not maintain the porosity of SCEs necessary to facilitate aqueous outflow, and the IOP may rise to the abnormal levels characteristic of many patients with glaucoma.

This study could not have been accomplished without the use of the F-D Nd:YAG laser, because this instrument, when applied using low-fluence light energy, preserves the baseline permeability properties of the lasered cells. Our results provide a new understanding of the mechanism of action of this novel glaucoma laser therapy based on the activities of the TMEs and SCEs, instead of purely mechanical effects.^{9,43} In view of the fact that laser effects appear to be cell-specific, we are inclined to support a more prominent role for the TMEs, which are most intensely activated by F-D Nd:YAG laser treatment. In addition, it is important to recall that the TMEs also release matrix metalloproteinases, which in promoting fluid flow across the extracellular matrix, also participate in facilitating the overall rate of aqueous outflow.¹⁰ It is also important to note that the interactions between TMEs and SCEs proceed in both directions and involve relationships within cells of a given type. This is important for several reasons. Interactions among TMEs allow for these cells to release factors that could affect the TMEs lining the outermost aqueous channels, which must be crossed before aqueous can pass into the juxtacanalicular tissues. The paracellular route of the outer TMEs is more porous than that in other TMEs lining the innermost trabecular meshwork beams and cords. Perhaps this particular widening of the paracellular route of TMEs lining the outermost trabecular meshwork is related to the cumulative effects of cytokines released by the entire population of TMEs becoming most concentrated, and having the greatest effect in TMEs near the juxtacanalicular tissues. Similarly, although the SCEs are less activated, factors released by these cells are particularly potent in promoting transendothelial flow across SCEs, as demonstrated by our experiments. Thus, the activation of SCEs by the laser treatment may be particularly effective in promoting transendothelial flow across the SCE barrier.

We conclude by noting that the use of the F-D Nd:YAG laser, and the in vitro methods described, has already allowed us to identify four cytokines released by lasered TMEs. Completion of this survey by identifying cytokines and chemokines involved, among the known 298 cytokines and chemokines, is a realistic goal, and such knowledge may enhance our future ability to manipulate aqueous outflow using some of these factors in the treatment of glaucoma.

REFERENCES

1. Hogan M, Alvarado J, Weddell J. *Histology of the Human Eye: An Atlas and Textbook*. Philadelphia: WB Saunders; 1971.
2. Alvarado JA, Betanzos A, Franse-Carman L, et al. Endothelia of Schlemm’s canal and trabecular meshwork: distinct molecular, functional, and anatomic features. *Am J Physiol Cell Physiol* 2004;286:C621-634.
3. Epstein DL, Rohen JW. Morphology of the trabecular meshwork and inner-wall endothelium after cationized ferritin perfusion in the monkey eye. *Invest Ophthalmol Vis Sci* 1991;32:160-171.
4. Bylsma SS, Samples JR, Acott TS, et al. Trabecular cell division after argon laser trabeculoplasty. *Arch Ophthalmol* 1988;106:544-547.
5. Alexander JP, Acott TS. Involvement of the Erk-MAP kinase pathway in TNFalpha regulation of trabecular matrix metalloproteinases and TIMPs. *Invest Ophthalmol Vis Sci* 2003;44:164-169.
6. Acott TS, Samples JR, Bradley JM, et al. Trabecular repopulation by anterior trabecular meshwork cells after laser trabeculoplasty. *Am J Ophthalmol* 1989;107:1-6.
7. Bradley JM, Anderssohn AM, Colvis CM, et al. Mediation of laser trabeculoplasty-induced matrix metalloproteinase expression by IL-1beta and TNFalpha. *Invest Ophthalmol Vis Sci* 2000;41:422-430.
8. Samples JR, Alexander JP, Acott TS. Regulation of the levels of human trabecular matrix metalloproteinases and inhibitor by interleukin-1 and dexamethasone. *Invest Ophthalmol Vis Sci* 1993;34:3386-3395.
9. Van Buskirk EM. Pathophysiology of laser trabeculoplasty. *Surv Ophthalmol* 1989;33:264-272.
10. Acott T, Wirtz M. Biochemistry of aqueous outflow. In: Krupin T, ed. *The Glaucomas*. St Louis: Mosby; 1996:281-305.
11. Alvarado JA, Franse-Carman L, McHolm G, et al. Epinephrine effects on major cell types of the aqueous outflow pathway: in vitro studies/clinical implications. *Trans Am Ophthalmol Soc* 1990;88:267-288.

12. Alvarado JA, Franse-Carman L, McHolm G, et al. The response of the meshwork cells to adrenergic agents and their antagonists. In: Krieglstein, ed. *Glaucoma Update IV*. Heidelberg, Germany: Springer Verlag; 1991:9-19.
13. Alvarado JA, Murphy CG, Franse-Carman L, et al. Effect of beta-adrenergic agonists on paracellular width and fluid flow across outflow pathway cells. *Invest Ophthalmol Vis Sci* 1998;39:1813-1822.
14. Alvarado JA, Wood I, Polansky JR. Human trabecular cells. II. Growth pattern and ultrastructural characteristics. *Invest Ophthalmol Vis Sci* 1982;23:464-478.
15. Underwood JL, Murphy CG, Chen J, et al. Glucocorticoids regulate transendothelial fluid flow resistance and formation of intercellular junctions. *Am J Physiol* 1999;277(2 pt 1):C330-342.
16. Yun AJ, Murphy CG, Polansky JR, et al. Proteins secreted by human trabecular cells. Glucocorticoid and other effects. *Invest Ophthalmol Vis Sci* 1989;30:2012-2022.
17. Polansky JR, Weinreb RN, Baxter JD, et al. Human trabecular cells. I. Establishment in tissue culture and growth characteristics. *Invest Ophthalmol Vis Sci* 1979;18:1043-1049.
18. Latina MA, Park C. Selective targeting of trabecular meshwork cells: in vitro studies of pulsed and CW laser interactions. *Exp Eye Res* 1995;60:359-371.
19. Latina M, Flotte T, Crean E, et al. Immunohistochemical staining of the human anterior segment. Evidence that resident cells play a role in immunologic responses. *Arch Ophthalmol* 1988;106:95-99.
20. Damji KF, Shah KC, Rock WJ, et al. Selective laser trabeculoplasty v argon laser trabeculoplasty: a prospective randomised clinical trial. *Br J Ophthalmol* 1999;83:718-722.
21. Anderson RR, Parrish JA. Selective photothermolysis: precise microsurgery by selective absorption of pulsed radiation. *Science* 1983;220(4596):524-527.
22. Perkins TW, Alvarado JA, Polansky JR, et al. Trabecular meshwork cells grown on filters. Conductivity and cytochalasin effects. *Invest Ophthalmol Vis Sci* 1988;29:1836-1846.
23. Barczak A, Rodriguez MW, Hanspers K, et al. Spotted long oligonucleotide arrays for human gene expression analysis. *Genome Res* 2003;13:1775-1785.
24. Ginzinger DG. Gene quantification using real-time quantitative PCR: an emerging technology hits the mainstream. *Exp Hematol* 2002;30:503-512.
25. Livak KJ, Schmittgen TD. Analysis of relative gene expression data using real-time quantitative PCR and the 2(-Delta Delta C(T)) method. *Methods* 2001;25:402-408.
26. Bolstad BM, Irizarry RA, Astrand M, et al. A comparison of normalization methods for high density oligonucleotide array data based on variance and bias. *Bioinformatics* 2003;19:185-193.
27. Irizarry RA, Bolstad BM, Collin F, et al. Summaries of Affymetrix GeneChip probe level data. *Nucleic Acids Res* 2003;31:e15.
28. Gentleman RC, Carey VJ, Bates DM, et al. Bioconductor: open software development for computational biology and bioinformatics. *Genome Biol* 2004;5:R80.
29. Smyth, GK. Linear models and empirical bayes methods for assessing differential expression in microarray experiments. *Statistical Applications in Genetics and Molecular Biology* [online] 2004;3(1):article 3.
30. Johnstone M, Grant WM. Pressure-dependent changes in structures of the aqueous outflow system of human and monkey eyes. *Am J Ophthalmol* 1973;75:365.
31. Mitton KP, Tumminia SJ, Arora J, et al. Transient loss of alphaB-crystallin: an early cellular response to mechanical stretch. *Biochem Biophys Res Commun* 1997;235:69-73.
32. Tumminia SJ, Mitton KP, Arora J, et al. Mechanical stretch alters the actin cytoskeletal network and signal transduction in human trabecular meshwork cells. *Invest Ophthalmol Vis Sci* 1998;39:1361-1371.
33. Gonzalez P, Epstein DL, Borrás T. Genes upregulated in the human trabecular meshwork in response to elevated intraocular pressure. *Invest Ophthalmol Vis Sci* 2000;41:352-361.
34. Borrás T, Rowlette LL, Tamm ER, et al. Effects of elevated intraocular pressure on outflow facility and TIGR/MYOC expression in perfused human anterior segments. *Invest Ophthalmol Vis Sci* 2002;43:33-40.
35. Epstein DL, Allingham RR, Schuman JS. *Chandler and Grant's Glaucoma*, 4th ed. Baltimore: Williams & Wilkins; 1997.
36. Alvarado JA, Murphy CG. Outflow obstruction in pigmentary and primary open angle glaucoma. *Arch Ophthalmol* 1992;110:1769-1778.
37. Alvarado JA, Murphy CG, Polansky J, et al. Age-related changes in trabecular meshwork cellularity. *Invest Ophthalmol Vis Sci* 1981;5:714-727.
38. Alvarado JA, Murphy CG, Juster R, et al. Studies on the pathogenesis of primary open angle glaucoma: regional analyses of trabecular meshwork cellularity and dense collagen. In: David R, Ticho U, eds. *Recent Advances in Glaucoma*. Amsterdam: Excerpta Medica; 1984:3-8.
39. Alvarado JA, Murphy CG, Juster R. Trabecular meshwork cellularity in primary open-angle glaucoma and nonglaucomatous normals. *Ophthalmology* 1984;91:564-579.
40. Murphy CG, Johnson M, Alvarado JA. Juxtacanalicular tissue in pigmentary and primary open angle glaucoma. The hydrodynamic role of pigment and other constituents. *Arch Ophthalmol* 1992;110:1779-1785.
41. Sacca SC, Pascotto A, Camicione P, et al. Oxidative DNA damage in the human trabecular meshwork: clinical correlation in patients with primary open-angle glaucoma. *Arch Ophthalmol* 2005;123:458-463.

42. Liu Y, Vollrath D. Reversal of mutant myocilin non-secretion and cell killing: implications for glaucoma. *Hum Mol Genet* 2004;13:1193-1204.
43. Van Buskirk EM, Pond V, Rosenquist RC, et al. Argon laser trabeculoplasty. Studies of mechanism of action. *Ophthalmology* 1984;91:1005-1010.

PEER DISCUSSION

DR RICHARD K. PARRISH II. To an ophthalmologist who has performed argon laser trabeculoplasty (ALT) for 25 years and selective laser trabeculoplasty (SLT) for 5 years without a genuine understanding of how either procedure lowers intraocular pressure, this presentation comes as a breath of fresh air. Dr Alvarado provides important new insight to explain the therapeutic effect of SLT by generating and meticulously testing a new hypothesis of trabecular meshwork function.

Initial attempts to explain how ALT works were based on an existing paradigm of trabecular meshwork physiology. Early discussions of increasing the traction on the trabecular beams as a result of light-tissue thermal reaction that increased the pore size never really seemed plausible, but provided at least a generation of ophthalmologist with some comfort as they reassured their patients that they knew what they were doing. More sophisticated studies involving the construct of the wounded trabecular meshwork endothelium (TME) healing itself in response to thermal injury by repopulating senescent cells to increase the turnover of juxtacanalicular proteoglycans was somewhat more satisfying. The most recent and progressively more specific investigation of cellular biologic events, including the expression of IL-1 alpha, IL-1 beta, and TNF still supported the notion of the self healing of the aging or injured TME after ALT.

Dr Alvarado breaks new ground by proposing a mechanism that not only explains how SLT lowers IOP, but also much more importantly how the trabecular and Schlemm's canal endothelia communicate to homeostatically regulate aqueous humor outflow. This does not mean that the previous studies on the thermally induced biologic effects of ALT are not relevant to that treatment, but that they do not explain SLT. The ultra short duration of light tissue interaction, 3 nanoseconds, does not result in direct cell death or initiate an apoptotic cascade based on histological findings or a genomic analysis of the laser conditioned media.

If the highest complement that can be paid to an engineer is describe his or her work as "elegant", then this adjective can be applied to the work presented today. If further studies define the exact composition of differentially expressed genes and their proteins, the impact will be to usher in a radically new era of therapeutic possibilities. I congratulate the authors on defining a promising new approach for rational glaucoma intervention.

DR JORGE A. ALVARADO. Dr Parrish adds important and appropriate background to this work in his remarks placing our new research findings in the context of prior theories of the mechanism of action of laser trabeculoplasty. Hopefully, future *in situ* and *in vivo* research will support our proposal as well indicating that the trabecular meshwork endothelial cells via the release of ligands modulate the permeability of Schlemm's canal endothelial cells, and that this trabecular endothelial cell driven mechanism is very much under the influence of circulating monocytes. These are tantalizing hypotheses because, respectively it (a) has long been believed that the juxtacanalicular connective tissues and the cellular barrier formed by the endothelial cells lining the lumen of Schlemm's canal constitute the mechanism; and (b) increasing evidence implicates the involvement of cells of inflammation, specifically mononuclear phagocytes (monocytes/macrophages) as a systemic mechanism participating in aqueous outflow homeostasis. I request that authorities refrain from having our residents choose the mechanism responsible for regulating aqueous outflow until the research is accomplished providing the scientific evidence to answer such questions appropriately.